

## **Micellar Aggregation and Membrane Partitioning of Bile Salts, Fatty Acids, Sodium Dodecyl Sulfate, and Sugar-Conjugated Fatty Acids: Correlation with Hemolytic Potency and Implications for Drug Delivery**

**Benjamin P. Ross,<sup>†</sup> April C. Braddy,<sup>‡</sup> Ross P. McGeary,<sup>†</sup> Joanne T. Blanchfield,<sup>†</sup> Laszlo Prokai,<sup>‡</sup> and Istvan Toth<sup>\*,†</sup>**

*School of Molecular and Microbial Sciences and School of Pharmacy, The University of Queensland, Brisbane, Queensland 4072, Australia, and Department of Medicinal Chemistry, College of Pharmacy, University of Florida, Gainesville, Florida 32610-0485*

Received February 24, 2004

**Abstract:** The co-administration of a drug with a penetration enhancer (PE) is one method by which the membrane permeability of a drug can be improved. To facilitate PE design, it is important that the molecular basis of PE toxicity and efficacy be examined, so we investigated the membrane affinity and micellar aggregation of a series of synthetic liposaccharide PEs and correlated these properties with hemolytic potency. The influence of liposaccharide alkyl chain length ( $n_c$ ) on the system was studied, and comparisons were made with conventional PEs such as bile salts, fatty acids, and surfactants. The liposaccharides were each synthesized in eight steps in good overall yield. Their critical micelle concentrations (CMCs) in phosphate-buffered saline ranged from 0.207 to 20.2 mM, and it was found that increasing  $n_c$  by 2 afforded a 1 order of magnitude decrease in the CMC. Immobilized artificial membrane (IAM) chromatography was used to determine each PE's affinity for biological membranes, and an increase in  $n_c$  caused a significant increase in the extent of membrane binding. A study of hemolytic activity revealed that liposaccharides with an  $n_c$  of  $\leq 12$  are the most likely to be biocompatible. The CMC values for all PEs showed a negative correlation with hemolytic potency; however, it was PE monomers, not micelles, that were responsible for the onset of hemolysis. The affinity of all enhancers for the IAM displayed a positive correlation with hemolytic potency, and therefore, IAM chromatography can be used to predict PE hemolytic activity. It was concluded that the biocompatibility of liposaccharides can be modulated by minor alterations in  $n_c$ .

**Keywords:** Penetration enhancer; absorption enhancer; drug delivery agent; excipient; synthesis; lipoamino acid; liposaccharide; sugar surfactant; CMC; ITC; hemolytic activity; IAM chromatography; biocompatibility; structure–property relationship

### **Introduction**

Many drugs must be administered via the parenteral route because poor gastrointestinal membrane permeability often precludes oral absorption. The parenteral route, however, has

disadvantages such as a greater risk of adverse events, patient discomfort, a higher drug product cost, the additional cost of equipment, and the time and expertise needed for administration.<sup>1,2</sup> Extensive research has therefore focused on methods of overcoming the poor membrane permeability of drugs. Some methods involve structural modification of

\* To whom correspondence should be addressed: School of Pharmacy, The University of Queensland, Brisbane, QLD 4072, Australia. Telephone: +61 7 3365 1386. Fax: +61 7 3365 1688. E-mail: i.toth@pharmacy.uq.edu.au.

<sup>†</sup> The University of Queensland.

<sup>‡</sup> University of Florida.

(1) *Therapeutic Guidelines Antibiotic*, 11th ed.; Therapeutic Guidelines Limited: North Melbourne, Australia, 2000.  
(2) Atkinson, H. C.; Chambers, S. T.; McGinlay, A. M. Antibiotic therapy costs. *N.Z. Med. J.* **1989**, *102*, 409–411.

the drug molecule, for example, conjugation with lipophilic or targeting moieties.<sup>3,4</sup> An alternative to structural modification is co-administration of the drug with a penetration enhancer, a substance that facilitates the transport of solutes across biological membranes.<sup>5</sup> Examples of penetration enhancers include surfactants, ion-pairing agents, fatty acids, bile salts, salicylates, saponins, calcium binding agents, and P-glycoprotein inhibitors.<sup>5–9</sup> One advantage of this approach is that the structural integrity and therefore biological activity of the drug are maintained. Some disadvantages are that many penetration enhancers perturb membrane lipids and proteins, thus causing damage to tissues,<sup>5,9</sup> and quite often toxicity is closely related to the mechanism by which an enhancer improves drug absorption.<sup>8</sup> For the progression of penetration enhancers to the clinic, biocompatible enhancers must be discovered, and biocompatibility stands alongside efficacy as a crucial factor in penetration enhancer design.<sup>5</sup>

Recently, we described<sup>10</sup> the application of a liposaccharide penetration enhancer (**7c**) to improve the gastrointestinal absorption of gentamicin, an aminoglycoside antibiotic with negligible (<1%) oral bioavailability. Rats treated orally with a mixture of **7c** (100 mg/kg) and gentamicin (60 mg/kg) showed a statistically significant increase in bioavailability when compared to control (60 mg of gentamicin/kg). Examination of the gastrointestinal tracts of the rats revealed no significant morphological changes to the tissues. Although the study gauged the efficacy of liposaccharide penetration enhancers, a quantitative measure of the biocompatibility of these enhancers was absent. In addition, it has been suggested<sup>5,11</sup> that to facilitate penetration enhancer design, it is important that studies examine the molecular basis of penetration enhancer toxicity and efficacy. In response to these needs, we examined the membrane affinity and micellar aggregation of a series of liposaccharide penetration enhancers (**7a–d**) and correlated these properties to hemolytic

potency (a measure of biocompatibility<sup>12–14</sup>). Variations of the alkyl chain length of the liposaccharides provided insight into the influence of this structural component on the system. For reference, comparison was made to conventional penetration enhancers such as the bile salts sodium deoxycholate (SDC) and sodium taurocholate (STC), the surfactant sodium dodecyl sulfate (SDS), and the fatty acids sodium decanoate (C10) and sodium dodecanoate (C12).

## Experimental Section

**General Procedures.** C10, C12, SDS, SDC, and STC were purchased from Sigma Chemical Company (St. Louis, MO). Phosphate-buffered saline (PBS) was prepared using PBS tablets (Amresco, Solon, OH) and contained 137 mM NaCl, 2 mM KCl, and 10 mM phosphate buffer (sodium and potassium phosphate salts) at pH 7.4. Commercial reagents were used without further purification. Flash column chromatography was performed using silica gel 60, 230–400 mesh (Scharlau, Barcelona, Spain). Thin-layer chromatography (TLC) was performed on silica gel 60 F<sub>254</sub> aluminum sheets (Merck, Darmstadt, Germany), and compounds were visualized with a ninhydrin dip (0.1% ninhydrin in ethanol) and heating. Melting points were measured with a capillary apparatus and are uncorrected. The mobile phase for mass spectrometry was solvent A (0.1% formic acid in water) and solvent B (0.1% formic acid in a 90% acetonitrile/10% water mixture). Mass spectra were recorded on a Perkin-Elmer Sciex API 3000 mass spectrometer operating in the positive-ion electrospray mode (ESI-MS) or an Applied Biosystems Qstar Pulsar electrospray qtof mass spectrometer operating in the positive-ion electrospray mode (HRMS), using 70% B at 0.3 mL/min. NMR spectra were recorded on either a Varian Gemini 300 instrument (300 MHz for <sup>1</sup>H and 75 MHz for <sup>13</sup>C) or a Bruker AM 500 instrument (500 MHz for <sup>1</sup>H and 125 MHz for <sup>13</sup>C). The following abbreviations were used to indicate the peak multiplicity: s, singlet; d, doublet; t, triplet; m, multiplet; br, broad. *J* values are in hertz. Proton signals were assigned using gradient COSY45 spectra recorded on the Bruker instrument. The synthesis of series **a** is described below. For the synthesis of series **b** and **d**, refer to the Experimental Section of the Supporting Information. The synthesis of **1b**<sup>15</sup> and series **c**<sup>10</sup> is reported elsewhere.

**2-(tert-Butoxycarbonylamino)-D,L-octanoic Acid (1a).** Sodium (3.18 g, 138 mmol) was dissolved in ethanol (100 mL) under nitrogen, and diethyl acetamido malonate (25.0

- (3) Tsuji, A.; Tamai, I. Carrier-mediated intestinal transport of drugs. *Pharm. Res.* **1996**, *13*, 963–977.
- (4) Wong, A.; Toth, I. Lipid, sugar and liposaccharide-based delivery systems. *Curr. Med. Chem.* **2001**, *8*, 1123–1136.
- (5) Lee, V. H.; Yamamoto, A.; Kompella, U. B. Mucosal penetration enhancers of facilitation of peptide and protein drug absorption. *Crit. Rev. Ther. Drug Carrier Syst.* **1991**, *8*, 91–192.
- (6) Muranishi, S. Absorption enhancers. *Crit. Rev. Ther. Drug Carrier Syst.* **1990**, *7*, 1–33.
- (7) Van Hoogdalem, E. J.; De Boer, A. G.; Breimer, D. D. Intestinal drug absorption enhancement: an overview. *Pharmacol. Ther.* **1989**, *44*, 407–443.
- (8) Aungst, B. J. Intestinal permeation enhancers. *J. Pharm. Sci.* **2000**, *89*, 429–442.
- (9) Swenson, E. S.; Curatolo, W. J. Intestinal permeability enhancement for proteins, peptides and other polar drugs: mechanisms and potential toxicity. *Adv. Drug Delivery Rev.* **1992**, *8*, 39–92.
- (10) Ross, B. P.; DeCruz, S. E.; Lynch, T. B.; Davis-Goff, K.; Toth, I. Design, synthesis, and evaluation of a liposaccharide drug delivery agent: application to the gastrointestinal absorption of gentamicin. *J. Med. Chem.* **2004**, *47*, 1251–1258.
- (11) Ganem-Quintanar, A.; Kalia, Y. N.; Falson-Rieg, F.; Buri, P. Mechanisms of oral permeation enhancement. *Int. J. Pharm.* **1997**, *156*, 127–142.
- (12) Gould, L. A.; Lansley, A. B.; Brown, M. B.; Forbes, B.; Martin, G. P. Mitigation of surfactant erythrocyte toxicity by egg phosphatidylcholine. *J. Pharm. Pharmacol.* **2000**, *52*, 1203–1209.
- (13) Bowe, C. L.; Mokhtarzadeh, L.; Venkatesan, P.; Babu, S.; Axelrod, H. R.; Sofia, M. J.; Kakarla, R.; Chan, T. Y.; Kim, J. S.; Lee, H. J.; Amidon, G. L.; Choe, S. Y.; Walker, S.; Kahne, D. Design of compounds that increase the absorption of polar molecules. *Proc. Natl. Acad. Sci. U.S.A.* **1997**, *94*, 12218–12223.
- (14) Miyamoto, E.; Murata, Y.; Kawashima, S.; Ueda, M. Haemolytic action of *N*-alkylpolymethylenediamines. *J. Pharm. Pharmacol.* **1992**, *44*, 269–271.

g, 115 mmol) was added, followed by 1-bromohexane (26.6 g, 161 mmol). The solution was refluxed overnight (ca. 18 h) under an atmosphere of nitrogen. Upon cooling, the mixture was poured onto crushed ice (600 mL), and the precipitated product was collected, air-dried, and then refluxed overnight (ca. 18 h) in a solution of concentrated HCl and *N,N*-dimethylformamide (DMF) (9:1, 200 mL). Upon cooling, the product precipitated and was collected, washed with ice-cold water, and then air-dried to afford 2-amino-D,L-octanoic acid hydrochloride (14.8 g, 66%): ESI-MS *m/z* 160 ([M + H]<sup>+</sup>).

2-Amino-D,L-octanoic acid hydrochloride (14.1 g, 72.2 mmol) was suspended in a solution of *tert*-butyl alcohol and water (2:3, 250 mL), and the pH was adjusted to 13 with sodium hydroxide (5 M). Di-*tert*-butyl dicarbonate (23.6 g, 108 mmol) in *tert*-butyl alcohol (50 mL) was added and the pH of the reaction maintained at 13 during the first 3 h by addition of sodium hydroxide (5 M). The solution was then left to stir overnight (ca. 18 h). The mixture was diluted with water (100 mL), and solid citric acid was added to acidify the mixture to pH 3. The mixture was extracted with ethyl acetate (4 × 150 mL), and the combined extracts were dried (MgSO<sub>4</sub>) and evaporated to yield a crude product which was recrystallized from acetonitrile to afford the title compound (**1a**, 11.5 g, 62%): mp 65–67 °C (lit.<sup>16</sup> mp 69–71 °C); ESI-MS *m/z* 260 ([M + H]<sup>+</sup>), 204 ([M – *tert*-butyl]<sup>+</sup>); <sup>1</sup>H NMR (300 MHz, CDCl<sub>3</sub>) δ 5.09 (1H, d, *J* = 7.5, CONH), 4.28 (1H, m, α-CH), 1.9–1.5 (2H, m, β-CH<sub>2</sub>), 1.41 [9H, s, C(CH<sub>3</sub>)<sub>3</sub>], 1.25 (8H, m, 4CH<sub>2</sub>), 0.84 (3H, t, *J* = 4.7, CH<sub>3</sub>); <sup>13</sup>C NMR (125 MHz, CDCl<sub>3</sub>) δ 177.5, 155.6, 80.0, 53.3, 32.4, 31.5, 28.8, 28.2, 25.1, 22.4, 13.9.

**2-(*tert*-Butoxycarbonylamino)-D,L-octanoic Acid Benzyl Ester (2a).** Carboxylic acid **1a** (1.96 g, 7.56 mmol) was dissolved in methanol (75 mL). The solution was neutralized (pH paper) with a 20% aqueous solution of Cs<sub>2</sub>CO<sub>3</sub> (ca. 7 mL) and the solvent removed *in vacuo*. DMF (30 mL) was added and the solvent removed *in vacuo*. Addition and evaporation of DMF (30 mL) were repeated to afford the solid cesium salt which was dried under reduced pressure. The cesium salt was dissolved in DMF (100 mL), and benzyl chloride (1.05 g, 0.95 mL, 8.29 mmol) was added. The mixture was stirred at 80 °C for 4 h. The solvent was removed *in vacuo* and the crude product taken up in ethyl acetate (200 mL) and washed with acid (5% HCl, 2 × 100 mL), saturated sodium bicarbonate (3 × 100 mL), and brine (100 mL). The organic layer was dried (MgSO<sub>4</sub>), filtered, and evaporated to afford the title compound (**2a**) as an oil (2.55 g, 97%): ESI-MS *m/z* 372 ([M + Na]<sup>+</sup>), 367 ([M +

NH<sub>4</sub>]<sup>+</sup>), 350 ([M + H]<sup>+</sup>), 294 ([M – *tert*-butyl]<sup>+</sup>), 250 ([M – Boc]<sup>+</sup>); <sup>1</sup>H NMR (500 MHz, CDCl<sub>3</sub>) δ 7.34 (5H, m, Ar-H), 5.16 (2H, m, Ar-CH<sub>2</sub>), 5.05 (1H, m, CONH), 4.33 (1H, m, α-CH), 1.77 (1H, m, β-CH), 1.61 (1H, m, β-CH), 1.43 [9H, s, C(CH<sub>3</sub>)<sub>3</sub>], 1.25 (8H, m, 4CH<sub>2</sub>), 0.86 (3H, t, *J* = 7.0, CH<sub>3</sub>); <sup>13</sup>C NMR (125 MHz, CDCl<sub>3</sub>) δ 172.7, 155.3, 135.5, 128.4, 128.2, 128.1, 79.6, 66.7, 53.5, 32.6, 31.4, 28.7, 28.2, 25.0, 22.4, 13.9; HRMS calcd for [M + H]<sup>+</sup> 350.2331, found 350.2343.

**2-Amino-D,L-octanoic Acid Benzyl Ester (3a).** Benzyl ester **2a** (2.08 g, 5.94 mmol) was dissolved in CH<sub>2</sub>Cl<sub>2</sub> and trifluoroacetic acid (40 mL, 1:1) and the mixture stirred for 1 h. The solvent was removed *in vacuo*, and the residue was dissolved in CH<sub>2</sub>Cl<sub>2</sub> (200 mL). The organic solution was washed with saturated sodium bicarbonate (2 × 200 mL) then dried (MgSO<sub>4</sub>), filtered, and evaporated to afford the title compound (**3a**) as an oil (1.27 g, 86%): ESI-MS *m/z* 250 ([M + H]<sup>+</sup>); <sup>1</sup>H NMR (500 MHz, CDCl<sub>3</sub>) δ 7.34 (5H, m, Ar-H), 5.16 (1H, d, *J* = 12.3, Ar-CH), 5.12 (1H, d, *J* = 12.3, Ar-CH), 3.46 (1H, m, α-CH), 1.71 (1H, m, β-CH), 1.58 (1H, m, β-CH), 1.25 (8H, m, 4CH<sub>2</sub>), 0.86 (3H, t, *J* = 7.0, CH<sub>3</sub>); <sup>13</sup>C NMR (125 MHz, CDCl<sub>3</sub>) δ 175.9, 135.7, 128.4, 128.1, 128.1, 66.3, 54.4, 34.8, 31.5, 28.9, 25.3, 22.3, 13.8; HRMS calcd for [M + H]<sup>+</sup> 250.1807, found 250.1814.

**N-[1-D,L-(Benzoyloxycarbonyl)heptyl]-1,2,3,4-tetra-O-acetyl-β-D-glucopyranuronamide (4a).** 1,2,3,4-Tetra-O-acetyl-β-D-glucopyranuronic acid<sup>10</sup> (1.51 g, 4.18 mmol) was dissolved in tetrahydrofuran (THF, 40 mL). Diisopropylethylamine (DIEA, 1.19 g, 1.60 mL, 9.20 mmol) and 2-(1H-benzotriazol-1-yl)-1,1,3,3-tetramethyluronium hexafluorophosphate (HBTU, 1.74 g, 4.60 mmol) were added, and the mixture was stirred for 10 min at room temperature. A solution of **3a** (0.937 g, 3.76 mmol) in THF (40 mL) was added, and the mixture was stirred overnight (ca. 18 h). The solvent was removed *in vacuo* to afford an oil which was taken up in CH<sub>2</sub>Cl<sub>2</sub> (200 mL) and washed with 5% HCl (2 × 200 mL), saturated sodium bicarbonate (2 × 200 mL), water (100 mL), and brine (100 mL). After being dried (MgSO<sub>4</sub>), the solvent was removed *in vacuo* to give an oil which was purified by silica flash column chromatography (ethyl acetate/hexane, 1:2) to afford the title compound (**4a**, a 1:1 mixture of diastereomers) as colorless crystals (2.17 g, 97%): mp 110–112 °C; TLC *R*<sub>f</sub> = 0.18 (ethyl acetate/hexane, 1:2); ESI-MS *m/z* 616 ([M + Na]<sup>+</sup>), 611 ([M + NH<sub>4</sub>]<sup>+</sup>), 594 ([M + H]<sup>+</sup>), 534 ([M – AcOH + H]<sup>+</sup>); <sup>1</sup>H NMR (500 MHz, CDCl<sub>3</sub>) δ 7.35 (5H, m, Ar-H), 6.82 (1H, m, amide NH), 5.79 (1H, m, H-1), 5.31 (1H, m, H-3), 5.24–5.10 (4H, m, overlapping Ar-CH<sub>2</sub>, H-2, H-4), 4.57 (1H, m, α-CH), 4.10 (1H, m, H-5), 2.12 (3H, m, Ac), 2.04 (6H, m, 2 Ac), 2.01 (3H, s, Ac), 1.81 (1H, m, β-CH), 1.68 (1H, m, β-CH), 1.23 (8H, m, 4CH<sub>2</sub>), 0.86 (3H, m, CH<sub>3</sub>); <sup>13</sup>C NMR (125 MHz, CDCl<sub>3</sub>) δ 171.7, 171.5, 169.7, 169.6, 169.3, 169.3, 169.1, 169.0, 168.7, 168.5, 165.6, 165.4, 135.3, 135.2, 128.5, 128.4, 128.2, 128.1, 91.3, 91.2, 73.1, 72.9, 72.0, 72.0, 70.2, 70.2, 69.0, 68.8, 67.1, 67.0, 51.9, 51.8, 32.2, 32.1, 31.4,

(15) Blanchfield, J. T.; Dutton, J. L.; Hogg, R. C.; Gallagher, O. P.; Craik, D. J.; Jones, A.; Adams, D. J.; Lewis, R. J.; Alewood, P. F.; Toth, I. Synthesis, structure elucidation, in vitro biological activity, toxicity, and caco-2 cell permeability of lipophilic analogues of α-conotoxin MII. *J. Med. Chem.* **2003**, *46*, 1266–1272.

(16) Kurita, M.; Atarashi, S.; Hattori, K.; Takano, T. Synthesis of 7-aminoacylamidocephalosporanic acids. *J. Antibiot., Ser. A* **1966**, *19*, 243–249.

31.3, 28.7, 28.6, 24.8, 24.7, 22.4, 22.3, 20.6, 20.6, 20.5, 20.5, 20.4, 13.9, 13.9; HRMS calcd for  $[M + H]^+$  594.2550, found 594.2703.

**N-[1-D,L-(Carboxy)heptyl]-1,2,3,4-tetra-O-acetyl- $\beta$ -D-glucopyranuronamide (5a).** Benzyl ester **4a** (1.33 g, 2.23 mmol) was dissolved in THF (40 mL). Pd/C catalyst (0.5 g, 10% Pd on C) was added, and the solution was stirred overnight (ca. 18 h) under an atmosphere of  $H_2$ . The mixture was filtered through Celite, and the solvent was evaporated *in vacuo* to give a solid which was purified by silica flash column chromatography (ethyl acetate/hexane, 3:2, acidified with 0.1% acetic acid) to afford the title compound (**5a**) as colorless crystals (0.80 g, 71%): mp 150–152 °C; TLC  $R_f$  = 0.10 (ethyl acetate/hexane, 3:2, 0.1% acetic acid),  $R_f$  = 0.26 (ethyl acetate, 0.1% acetic acid); ESI-MS  $m/z$  526 ( $[M + Na]^+$ ), 521 ( $[M + NH_4]^+$ ), 504 ( $[M + H]^+$ ), 444 ( $[M - AcOH + H]^+$ );  $^1H$  NMR (500 MHz,  $CDCl_3$ )  $\delta$  7.89 (1H, br s, COOH), 6.81 (1H, m, amide NH), 5.78 (1H, m, H-1), 5.30 (1H, m, H-3), 5.24–5.10 (2H, m, overlapping H-2, H-4), 4.51 (1H, m,  $\alpha$ -CH), 4.15 (1H, m, H-5), 2.13 (3H, m, Ac), 2.03 (6H, m, 2Ac), 2.00 (3H, m, Ac), 1.86 (1H, m,  $\beta$ -CH), 1.70 (1H, m,  $\beta$ -CH), 1.28 (8H, m, 4CH<sub>2</sub>), 0.86 (3H, m, CH<sub>3</sub>);  $^{13}C$  NMR (125 MHz,  $CDCl_3$ )  $\delta$  175.4, 175.2, 169.9, 169.8, 169.6, 169.5, 169.3, 168.7, 166.1, 166.1, 91.4, 91.3, 73.0, 72.9, 72.1, 72.0, 70.3, 70.2, 69.0, 68.9, 51.9, 51.8, 31.9, 31.4, 31.4, 28.8, 28.7, 25.0, 24.9, 22.5, 22.4, 20.7, 20.7, 20.5, 20.5, 20.4, 13.9, 13.9; HRMS calcd for  $[M + H]^+$  504.2081, found 504.2099.

**N-[1-D,L-(Carboxy)heptyl]- $\alpha$ , $\beta$ -D-glucopyranuronamide (6a).** Compound **5a** (0.780 g, 1.55 mmol) was dissolved in methanol (30 mL). A sodium methoxide solution (30 mL, 0.2 M) was added, and the solution was stirred at room temperature for 2 h. The mixture was neutralized with ion-exchange resin [Amberlite IR-120 ( $H^+$ )] and filtered, and then the solvent was removed *in vacuo*. The product was lyophilized from acetonitrile and water (1:1) to afford the title compound (**6a**, 0.481 g, 93%): ESI-MS  $m/z$  671 ( $[2M + H]^+$ ), 336 ( $[M + H]^+$ );  $^1H$  NMR (500 MHz,  $d_6$ -DMSO)  $\delta$  8.0–7.5 (1H, m, amide NH), 4.4–2.9 (m), 1.71 (1H, m,  $\beta$ -CH), 1.62 (1H, m,  $\beta$ -CH), 1.25 (8H, m, 4CH<sub>2</sub>), 0.85 (3H, t,  $J$  = 6.7, CH<sub>3</sub>); HRMS calcd for  $[M + H]^+$  336.1658, found 336.1652.

**Sodium N-[1-D,L-(Carboxy)heptyl]- $\alpha$ , $\beta$ -D-glucopyranuronamide (7a).** The free acid **6a** (0.464 g, 1.38 mmol) was suspended in acetonitrile and water (30 mL, 1:2 solution), and aqueous sodium bicarbonate (2.77 mL, 0.5 M solution, 1.38 mmol) was added. The mixture was sonicated until a clear solution was obtained. The solution was lyophilized to afford the title compound (**7a**) in quantitative yield (0.495 g): ESI-MS  $m/z$  693 ( $[2M + Na]^+$ ), 358 ( $[M + Na]^+$ ), 336 ( $[M + H]^+$ );  $^1H$  NMR (500 MHz,  $d_6$ -DMSO)  $\delta$  7.55 (1H, m, amide NH), 4.4–2.9 (m), 1.68 (1H, m,  $\beta$ -CH), 1.51 (1H, m,  $\beta$ -CH), 1.20 (8H, m, 4CH<sub>2</sub>), 0.84 (3H, t,  $J$  = 6.8, CH<sub>3</sub>); HRMS calcd for  $[M + Na]^+$  358.1478, found 358.1485.

**Isothermal Titration Microcalorimetry.** Isothermal titration microcalorimetry (ITC) was performed using a MicroCal VP-ITC titration calorimeter (MicroCal, Northamp-

ton, MA) at 37 °C. To ensure the solubility of C10 and C12, experiments using these compounds were conducted at 50 °C. Test solutions were prepared by dissolving a sample of the penetration enhancer in PBS to afford an accurate penetration enhancer concentration that was well above the CMC. The solutions were then sonicated for at least 10 min at ca. 40 °C. The solutions of C10 and C12 were sonicated at ca. 55 °C to aid solubilization. The reaction cell (1.4395 mL) was loaded with PBS. Aliquots of the PBS solution of the penetration enhancer were injected into the reaction cell at regular intervals using a 300  $\mu$ L injection/stirrer syringe rotating at 300 rpm. The specific parameters for each study were as follows {compound [concentration in syringe (millimolar), number of injections, injection volume (microliters), injection duration (seconds), injection spacing (minutes)]}: **7b** [220, 94, 3, 6, 6], **7c** [40, 87, 3, 6, 6],<sup>10</sup> **7d** [4, 87, 3, 6, 6], C10 [450, 54, 5, 10, 10], C12 [30, 54, 5, 10, 8], SDS [25, 54, 5, 10, 6], SDC [90, 54, 5, 10, 6], and STC [170, 40, 7, 14, 8]. All experiments were performed in triplicate, except for those with **7b** which were carried out in duplicate due to the limited availability of the compound. Origin (version 5.0, Microcal) and Microsoft Excel 2002 (Microsoft, WA) were used for data analysis.

**Hemolytic Activity Assay.** The penetration enhancers were serially diluted in PBS to give 100  $\mu$ L test solutions in 96-well round-bottom microtiter plates. All compounds were readily soluble in PBS (the maximum concentration that was examined was 40 mM). Blood was collected from an individual Caucasian male subject and added to heparinized tubes. Following centrifugation (2200g for 10 min), the plasma and buffy coat were removed, and the packed red cells were resuspended in PBS to ca. 3 times their packed volume. The suspension was centrifuged (2200g for 10 min) and the supernatant removed. The washing cycle of suspension in PBS, centrifugation, and removal of supernatant was repeated (ca. three times) until a clear supernatant was obtained. The clear supernatant was removed, and the packed red cells were resuspended in PBS to a volume equivalent to 3 times the original whole blood volume. The microtiter plates and the washed red cell suspension were placed in a 37 °C incubator (Heidolf Titramax/Incubator 1000, Heidolf Instruments, Cinnaminson, NJ). After a 15 min incubation, an aliquot (100  $\mu$ L) of the washed red cell suspension was added to each of the microtiter plate wells that contained the test solutions. The microtiter plates were incubated for 15 min at 37 °C while being shaken at 300 rpm (Heidolf Titramax/Incubator 1000). The plates were centrifuged (1500g for 10 min), and an aliquot (20  $\mu$ L) of supernatant was removed from each well and added to the individual wells of a 96-well flat-bottom microtiter plate which contained 180  $\mu$ L of Drabkin's Agent (1.25 g in 1 L of water) per well. The flat-bottom plate was stored in the dark for 1 h, and then the absorbance of each well was measured at 570 nm using a microplate reader (Bio-Rad 550, Bio-Rad Laboratories, Hercules, CA). The percent hemolysis was calculated as the percentage of maximum lysis (80 mM SDS in PBS control) after correction for spontaneous lysis (PBS

control), using the equation<sup>15</sup>

$$\% \text{ hemolysis} = \frac{\text{Abs}_{570} - \text{minAbs}_{570}}{\text{maxAbs}_{570} - \text{minAbs}_{570}} \times 100 \quad (1)$$

where  $\text{Abs}_{570}$ ,  $\text{maxAbs}_{540}$ , and  $\text{minAbs}_{540}$  are the absorbance values of the test solution, 80 mM SDS in PBS control, and PBS control, respectively. The concentration of penetration enhancer required to cause 10% hemolysis ( $\text{EC}_{10}$ ) was calculated by linear regression of three data points spanning the 10% hemolysis value in a plot of percent hemolysis versus penetration enhancer concentration.

**Immobilized Artificial Membrane (IAM) Chromatography.** Determination of the capacity factors ( $k'_{\text{IAM}}$ ) of the penetration enhancers was carried out using a 3 cm  $\times$  4.6 mm (inside diameter) IAM.PC.DD2 column packed with 5  $\mu\text{m}$  particles (Regis Technologies, Morton Grove, IL) and protected with a 1 cm  $\times$  3.0 mm (inside diameter) guard cartridge. Dulbecco's phosphate-buffered saline (8.1 mM  $\text{Na}_2\text{HPO}_4$ , 1.5 mM  $\text{KH}_2\text{PO}_4$ , 136.9 mM NaCl, and 2.7 mM KCl) adjusted to pH 7.4 with potassium hydroxide and fortified, if necessary, with a varying percentage of acetonitrile (in 5% increments) was used as a mobile phase at a flow rate of 1.0 mL/min. UV chromatograms were obtained at 205 nm using a Hewlett-Packard 1050 high-performance liquid chromatograph equipped with a diode-array detector and autosampler (Agilent, Palo Alto, CA). The compounds were dissolved in deionized water to give 1.0 mg/mL solutions, and 25  $\mu\text{L}$  of the solution was injected for analysis. The void [ $t_{\text{R}(0)}$ ] marker was the tripeptide pGlu-Glu-Pro-NH<sub>2</sub> that manifested practically no affinity to the IAM stationary phase,<sup>17</sup> and the  $k'_{\text{IAM}}$  capacity factor was calculated using the equation

$$k'_{\text{IAM}} = [t_{\text{R}(\text{X})} - t_{\text{R}(0)}]/t_{\text{R}(0)} \quad (2)$$

where  $t_{\text{R}(\text{X})}$  and  $t_{\text{R}(0)}$  are the retention times for the penetration enhancer and void marker, respectively [see Figure S2A of the Supporting Information for a sample IAM chromatogram that indicates retention time reproducibility ( $\text{SD} < 2\%$ )]. To allow for a direct comparison of affinities for the IAM, the  $k'_{\text{IAM}}$  values obtained from isocratic elutions with various concentrations of the organic modifier were extrapolated to a purely aqueous condition using linear regression (see Figure S2B of the Supporting Information which illustrates the procedure using **7c** as an example).

## Results and Discussion

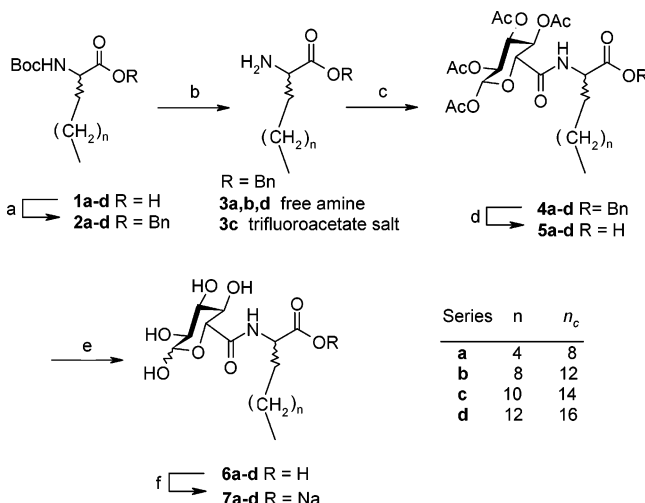
**Theory of Molecular Design.** Most penetration enhancers are endogenous substances (e.g., bile salts, fatty acids) or were designed for purposes other than drug delivery (e.g., calcium binding agents and many surfactants).<sup>5–9</sup> It has been suggested<sup>5,11</sup> that research must be directed toward the design

of penetration enhancers for drug delivery, and improved efficacy and biocompatibility must be a focus of design. Liposaccharides **7** are synthetic constructs created with such goals in mind. As reported previously,<sup>10</sup> they are designed to possess the combined properties of successful penetration enhancers such as surfactants<sup>9</sup> and ion-pairing agents,<sup>18</sup> and to increase biocompatibility, they are constructed from natural body constituents, namely, sugars and fatty acids. Fatty acids are effective penetration enhancers,<sup>6–8</sup> and sodium decanoate is one of the few penetration enhancers to have gained regulatory approval.<sup>19</sup> Hence, further examination of the fatty acid series as penetration enhancers is warranted. In addition, it has been reported that fatty acids with alkyl chains longer than sodium dodecanoate may be effective as penetration enhancers, but because of their low water solubility, these are often combined with emulsifying agents.<sup>6,8</sup> For liposaccharides **7**, conjugation of a lipoamino acid (LAA, **3**, R = H) with a hydrophilic D-glucopyranuronic acid (GlcA) moiety improves the water solubility of the lipid and so affords water-soluble long chain fatty acid derivatives.

It is worth noting that liposaccharides **7** may be classified as “sugar surfactants” because they possess a hydrophilic sugar moiety (the GlcA) linked to a hydrophobic alkyl chain (the LAA). Sugar surfactants are used in cosmetic, manual dishwashing, and food emulsifying applications, because they typically display nonaggressive character against living matter,<sup>20–22</sup> a property that is integral to drug delivery applications. The hydrophilic group of conventional sugar surfactants consists of either a nonionic sugar (e.g., alkyl glycosides<sup>23</sup>) or an ionic sugar with the charge located on the pyranose ring (e.g., sugar sulfonates,<sup>24</sup> sulfated sugars,<sup>25,26</sup>

- (18) Quintanar-Guerrero, D.; Allemann, E.; Fessi, H.; Doelker, E. Applications of the ion-pair concept to hydrophilic substances with special emphasis on peptides. *Pharm. Res.* **1997**, *14*, 119–127.
- (19) Lindmark, T.; Soderholm, J. D.; Olaison, G.; Alvan, G.; Ocklind, G.; Artursson, P. Mechanism of absorption enhancement in humans after rectal administration of ampicillin in suppositories containing sodium caprate. *Pharm. Res.* **1997**, *14*, 930–935.
- (20) Hill, K.; Rhode, O. Sugar-based surfactants for consumer products and technical applications. *Fett/Lipid* **1999**, *101*, 25–33.
- (21) Boullanger, P.; Chevalier, Y. Surface active properties and micellar aggregation of alkyl 2-amino-2-deoxy- $\beta$ -D-glucopyranosides. *Langmuir* **1996**, *12*, 1771–1776.
- (22) Savelli, M. P.; Van Roekeghem, P.; Douillet, O.; Cave, G.; Gode, P.; Ronco, G.; Villa, P. Effects of tail alkyl chain length (n), head group structure and junction (Z) on amphiphilic properties of 1-Z-R-D,L-xylitol compounds (R = C<sub>n</sub>H<sub>2n+1</sub>). *Int. J. Pharm.* **1999**, *182*, 221–236.
- (23) von Rybinski, W.; Hill, K. Alkyl polyglycosides: properties and applications of a new class of surfactants. *Angew. Chem., Int. Ed.* **1998**, *37*, 1328–1345.
- (24) Fernandez-Bolanos, J.; Maya Castilla, I.; Fernandez-Bolanos Guzman, J. Surfactants. Part XIII. Syntheses of sodium 2-(acylamino)-2,6-dideoxy-D-glucopyranose-6-sulfonates. *Carbohydr. Res.* **1988**, *173*, 33–40.
- (25) Bazito, R. C.; El Seoud, O. A. Sugar-based anionic surfactants: synthesis and micelle formation of sodium methyl 2-acylamido-2-deoxy-6-O-sulfo-D-glucopyranosides. *Carbohydr. Res.* **2001**, *332*, 95–102.

(17) Prokai-Tatrai, K.; Nguyen, V.; Zharikova, A. D.; Braddy, A. C.; Stevens, S. M.; Prokai, L. Prodrugs to enhance central nervous system effects of the TRH-like peptide pGlu-Glu-Pro-NH<sub>2</sub>. *Bioorg. Med. Chem. Lett.* **2003**, *13*, 1011–1014.

Scheme 1<sup>a</sup>

<sup>a</sup> Reagents and conditions: (a) (i)  $\text{Cs}_2\text{CO}_3$ , MeOH; (ii)  $\text{BnCl}$ , DMF,  $80^\circ\text{C}$ , 4 h; (b)  $\text{CF}_3\text{COOH}$ ,  $\text{CH}_2\text{Cl}_2$ , 1 h; (c) 1,2,3,4-tetra-O-acetyl- $\beta$ -D-glucopyranuronic acid,<sup>10</sup> HBTU, DIPEA, THF, 18 h; (d)  $\text{H}_2$ , 10%  $\text{Pd/C}$ , THF, 18 h; (e) (i) 0.1 M  $\text{NaOMe}$ , MeOH, 2 h; (ii) Amberlite IR-120 ( $\text{H}^+$ ); (f)  $\text{NaHCO}_3$ .  $n_c$  is the number of carbon atoms in the lipoamino acid or fatty acid.

amino sugars,<sup>27</sup> and quaternary ammonium sugars<sup>28</sup>). The structure of liposaccharides **7** however is unique, because they possess a voluminous headgroup which consists of not only the nonionic GlcA moiety but also an ionized carboxylic acid group that is not directly attached to the pyranose ring. Such a novel structure promotes interest in the aggregation properties of series **7**.

**Synthesis.** The synthetic pathway to **7a-d** is outlined in Scheme 1. Variations of the alkyl chain length were achieved simply by selecting the appropriate alkyl bromide for the preparation of **1a-d**. The subsequent synthetic steps adhered to the literature procedures,<sup>10</sup> except for compounds **3a,b,d**, which were isolated as the free base rather than the trifluoroacetate salt. Overall, each liposaccharide (**7a-d**) was synthesized in eight steps in good yield.

**Critical Micelle Concentration.** The critical micelle concentration (CMC)<sup>29-31</sup> is an important physicochemical parameter which can help to explain the interaction between an amphiphile and a drug or biological system. To elucidate

structure–property relationships, it is essential to know whether an amphiphile is in the monomer or aggregated state. For example, the amphiphile-assisted solubilization of hydrophobic drugs in aqueous solution is dependent on the existence of a hydrophobic micelle core which can entrap the drug, and therefore, solubilization occurs only above the CMC.<sup>31</sup> A similar mechanism, involving solubilization of insulin by the formation of insulin/bile salt mixed micelles, is believed to be responsible for the correlation between bile salt CMC and the ability of various bile salts to enhance nasal insulin absorption.<sup>32</sup> In the same study, the differing efficacy of various bile salts as penetration enhancers was attributed to their differing capacities to aggregate as reverse micelles within cell membranes and form transmembrane channels. Bowe et al.<sup>13</sup> observed that glycosylated bile salts were effective only at concentrations above their CMCs, although no correlation between CMC and efficacy was observed. Knowledge of the CMC can also provide insight into the potential toxicity of a penetration enhancer because micelles may extract membrane lipids and proteins to form mixed micelles.<sup>9</sup>

In this study, we characterized the CMC of the penetration enhancers using isothermal titration microcalorimetry (ITC).<sup>33</sup> ITC is a sensitive method that is routinely used to characterize the CMC and the thermodynamics of micellar aggregation.<sup>33,34</sup> Aliquots of a solution containing micelles of a penetration enhancer, in PBS at pH 7.4, were injected into a microcalorimeter sample cell loaded with a PBS solution, and the enthalpy change associated with each addition was measured. Figure 1A is a plot of reaction enthalpy ( $\Delta H$ ) as a function of the concentration ( $c$ ) of **7d** in the sample cell. Figure 1A is typical of the penetration enhancer  $\Delta H$  versus  $c$  plots obtained in this study. The plot may be divided into two regions within which the enthalpies are similar. For the first portion of the curve (Figure 1A,  $c < c_1$ ), the measured enthalpy changes are ascribed to demicellization (the breaking up of micelles into monomers). Once the concentration of **7d** in the sample cell passes the CMC, the measured enthalpy changes represent the dilution enthalpy of the micelle (Figure 1A,  $c > c_3$ ).<sup>35</sup> The CMC is a concentration between these two regions of the curve (i.e.,  $c_1 \leq \text{CMC} \leq c_3$ ).

(26) Bazito, R. C.; El Seoud, O. A. Sugar-based surfactants: adsorption and micelle formation of sodium methyl 2-acylamido-2-deoxy-6-O-sulfo-D-glucopyranosides. *Langmuir* **2002**, *18*, 4362–4366.

(27) Matsumura, S.; Kawamura, Y.; Yoshikawa, S.; Kawada, K.; Uchibori, T. Surface activities, biodegradability and antimicrobial properties of glucosamine derivatives containing alkyl chains. *J. Am. Oil Chem. Soc.* **1993**, *70*, 17–22.

(28) Bazito, R. C.; El Seoud, O. A. Sugar-based cationic surfactants: synthesis and aggregation of methyl 2-acylamido-6-trimethylammonio-2,6-dideoxy-D-glucopyranoside chlorides. *J. Surfactants Deterg.* **2001**, *4*, 395–400.

(29) Clint, J. H. *Surfactant Aggregation*; Blackie: London, 1992.

(30) Rosen, M. J. *Surfactants and Interfacial Phenomena*, 2nd ed.; Wiley: New York, 1989.

(31) Attwood, D.; Florence, A. T. *Surfactant Systems: their chemistry, pharmacy, and biology*; Chapman and Hall: London, 1983.

(32) Gordon, G. S.; Moses, A. C.; Silver, R. D.; Flier, J. S.; Carey, M. C. Nasal absorption of insulin: enhancement by hydrophobic bile salts. *Proc. Natl. Acad. Sci. U.S.A.* **1985**, *82*, 7419–7423.

(33) Blandamer, M. J.; Cullis, P. M.; Engberts, J. B. F. N. Titration microcalorimetry. *J. Chem. Soc., Faraday Trans.* **1998**, *94*, 2261–2267.

(34) Paula, S.; Sus, W.; Tuchtenhagen, J.; Blume, A. Thermodynamics of micelle formation as a function of temperature: a high-sensitivity titration calorimetry study. *J. Phys. Chem.* **1995**, *99*, 11742–11751.

(35) van Os, N. M.; Daane, G. J.; Haandrikman, G. The effect of chemical structure upon the thermodynamics of micellization of model alkylarenesulfonates. III. Determination of the critical micelle concentration and the enthalpy of demicellization by means of microcalorimetry and a comparison with the phase separation model. *J. Colloid Interface Sci.* **1991**, *141*, 199–217.

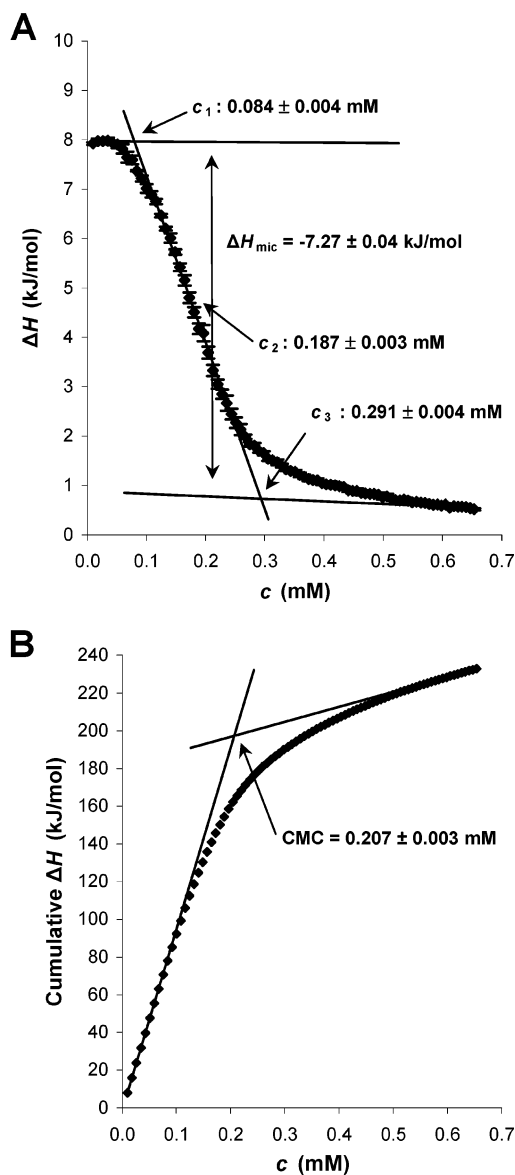


**Figure 1.** (A) Molar reaction enthalpy as a function of the total concentration of **7d** in the sample cell as observed during the titration of a micellar PBS solution of **7d** (4 mM, 3  $\mu$ L steps) into 1.4 mL of PBS at 37 °C. Values are the mean  $\pm$  SEM of three replicate titrations. The enthalpy of micellization is represented by the length of the double-headed arrow.  $c_1$ – $c_3$  describe the concentrations of the transition region. (B) van Os plot for **7d**. Cumulative molar reaction enthalpy as a function of the total concentration of **7d** in the sample cell for the experiment presented in panel A. The CMC is defined as the concentration at which the two lines, fitted by linear regression to data well above and below the discontinuity in the curve, intersect. Values are the mean of three replicate titrations with a percent relative SEM of <2%. The CMC is displayed as the mean  $\pm$  SEM.

$c_3$ ) and can be estimated by various methods.<sup>34–36</sup> For amphiphiles which exhibit an abrupt change in enthalpy upon micellization, the method used to estimate CMC has little influence on the CMC value. However, for those surfactants

**Table 1.** Penetration Enhancer CMC Values Estimated from  $\Delta H$  versus  $c$  Data

compound	van Os method	CMC <sup>a</sup> (mM)		
		linear regression method		
		$c_1$	$c_2$	$c_3$
<b>7b<sup>b</sup></b>	20.2	12.6	19.1	25.6
<b>7c</b>	2.09 <sup>c</sup>	0.97	1.89	2.80
<b>7d</b>	0.207	0.084	0.187	0.291
STC <sup>d</sup>	12.5	6.03	11.1	16.2
C10 <sup>e,f</sup>	–	37.8	–	–
SDC <sup>d</sup>	4.58	2.37	3.93	5.50
C12 <sup>d,e</sup>	3.15 <sup>g</sup>	2.66	3.08	3.49
SDS <sup>d</sup>	1.28	1.07	1.23	1.34

<sup>a</sup> Values are the mean of three replicate titrations with a percent relative SEM of <5%. All experiments were performed in PBS at 37 °C. Note exceptions b and e which follow. <sup>b</sup> Performed in duplicate. <sup>c</sup> Reported previously.<sup>10</sup> <sup>d</sup> Lit. CMC: 9 mM for STC (35 °C, 0.15 M NaCl, dye solubilization),<sup>70</sup> 3.8 mM for SDC (35 °C, 0.1 M NaCl, ITC),<sup>46</sup> 11 mM for C12 (50 °C, 0.1 N NaCl, dye solubilization),<sup>71</sup> and 1.54 mM for SDS (25 °C, 0.1 M NaCl, ITC).<sup>34</sup> <sup>e</sup> Performed at 50 °C. <sup>f</sup> Type C enthalpogram<sup>69</sup> (see Figure S1 of the Supporting Information); therefore, only  $c_1$  is a suitable estimate of the CMC. <sup>g</sup>  $\Delta H$  changes sign during the titration experiment; therefore,  $\Delta H$  values were transformed by 5 kJ/mol prior to estimation of the CMC.

which have broad transition regions, for example, bile salts,<sup>34</sup> appreciable variation in CMC values may exist depending on the method used to estimate CMC. Such discrepancies motivated us to determine the CMC values for our system with the aid of the two methods described below.

The CMC of **7c** (2.09 mM) was recently estimated<sup>10</sup> using the method of van Os<sup>35</sup> in which the cumulative enthalpy was plotted as a function of surfactant concentration (van Os plot). Figure 1B is the van Os plot for **7d**. This figure shows a change of slope about the CMC, the value of which was calculated by selecting data well below and above the CMC, fitting these to a pair of straight lines by linear regression, and taking their point of intersection as the CMC.<sup>35</sup> Using this method, the CMC value approximates the concentration at the inflection point of a  $\Delta H$  versus  $c$  plot (Figure 1A). Table 1 lists the penetration enhancer CMC values estimated from van Os plots.

The concentration at the inflection point in a  $\Delta H$  versus  $c$  plot represents the concentration at which the rate of micelle formation is maximal.<sup>36</sup> It has been noted<sup>36</sup> that this is at variance with the meaning of the CMC which is regarded as the concentration at which micellization first begins.<sup>37</sup> In accordance with this definition, the CMC was also estimated as the point of intersection of the lines extrapolated from the linear regions on either side of the first discontinuity in a  $\Delta H$  versus  $c$  plot ( $c_1$  in Figure 1A).<sup>36,38</sup> Table 1 lists the penetration enhancer CMC values calculated by this method

(36) Shackleford, D. M.; Pranker, R. J.; Scanlon, M. J.; Charman, W. N. Self-Micellization of Gemfibrozil 1- $\beta$  Acyl Glucuronide in Aqueous Solution. *Pharm. Res.* **2003**, *20*, 465–470.  
 (37) Mukerjee, P.; Mysels, K. J. *Critical Micelle Concentrations of Aqueous Surfactant Systems*; U.S. National Bureau of Standards: Washington, DC, 1971.

( $c_1$  values). As an extension of this method, we provide additional descriptors of the  $\Delta H$  versus  $c$  plots, namely, points  $c_2$  and  $c_3$  (Figure 1A and Table 1).  $c_3$  is the concentration at the point of intersection of the lines extrapolated from the linear regions on either side of the second discontinuity in Figure 1A. The concentration at the midpoint of the  $c_1$ – $c_3$  line is  $c_2$ . These values ( $c_1$ – $c_3$ ) provide a simple, quantitative description of the transition region of the  $\Delta H$  versus  $c$  plot, and they are particularly useful in characterizing the micellization of surfactants with broad transition ranges, for which a single concentration point description (the CMC) is inadequate. In fact, the range of  $c_1$ – $c_3$  quantifies the “critical concentration range” that has been described qualitatively by others.<sup>34</sup> Unless stated otherwise, future discussion of CMC in this paper refers to the CMC value determined by the method of van Os.

Table 1 indicates that liposaccharides **7b** and **7c** have CMC values in the range of conventional bile salt (STC and SDC) and fatty acid (C10 and C12) penetration enhancers, whereas the CMC of **7d** is 1 order of magnitude lower. Comparison of the CMC of **7b** (20.2 mM) with the CMC of the structurally similar fatty acid C12 (3.15 mM) reveals that sugar conjugation increases the CMC by a factor of 6. It is known<sup>30</sup> that the introduction of polar groups into the hydrophobic tail of surfactants generally causes a significant increase in the CMC since carbon atoms between the polar group and the hydrophilic head have a weaker effect on the CMC (when compared to their effect were the polar group absent). Therefore, in **7b**–**d**, the LAA carbonyl and  $\alpha$ -carbon atom have little influence on the CMC, and **7b**–**d** effectively have 10, 12, and 14 carbon atoms, respectively, in their hydrophobic tail. Hence, the CMC of **7b** (20.2 mM) and the CMC of C10 (37.8 mM) differ by a factor of only 2. Likewise, **7c**, which effectively has 12 carbons in its hydrophobic tail, and C12 have similar CMC values of 2.09 and 3.15 mM, respectively.

The relationship (Figure 2) between log CMC and the number of LAA carbon atoms ( $n_c$ ) for **7b**–**d** adheres to the empirical Klevens equation<sup>39,40</sup> ( $\log \text{CMC} = a - bn_c$ ). The magnitude of  $b$  is characteristic of the surfactant type, and  $b$  is ca. 0.3 for ionics,<sup>30</sup> which means that the CMC decreases by a factor of 4 for each two methylenes added to the hydrophobic tail. For the ionic surfactants **7b**–**d**, however,  $b$  is 0.50 which means that for each two methylenes added to the LAA moiety, the CMC decreases by a factor of 10. Such a value of  $b$  is expected for nonionics and zwitterionics (for which  $b \sim 0.5$ ),<sup>30</sup> but not for the ionic series **7b**–**d**. This anomaly is attributed to the presence of added salt (NaCl, KCl, and buffer salts) which shields the ionic

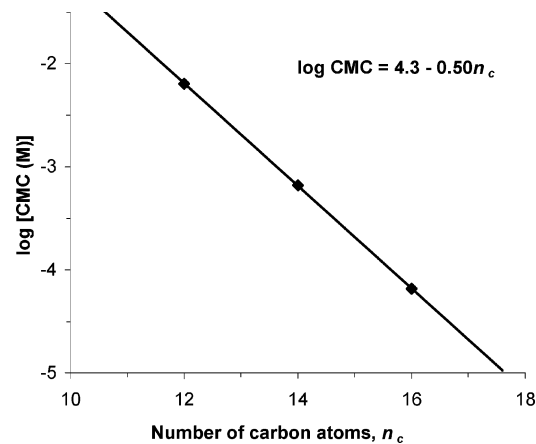


**Figure 2.** Variation of the log CMC with the number of LAA carbon atoms ( $n_c$ ) for the series **7b**–**d**.

headgroups. (For explanations of the salt effect, the reader is referred to Tanford<sup>41</sup> and Shinoda,<sup>42</sup> and discussion is provided in the Results and Discussion of the Supporting Information.) Such a salt effect has been reported;<sup>41,43</sup> however, the implications for drug delivery applications have not been emphasized. The implications are that for ionic surfactants in isotonic media, lengthening the hydrophobic tail by two methylenes causes a 1 order of magnitude decrease in CMC, not the factor of 4 reduction that is commonly observed for low-ionic strength media.<sup>29,30</sup> Thus, for *both* nonionic and ionic penetration enhancers, with hydrophobic tails, it is possible to significantly vary the CMC through only *minor* alterations of the alkyl chain length, and therefore, it may also be possible to precisely modulate efficacy and toxicity.

In summary, **7b** and **7c** have CMC values in the range of those of conventional bile salt (STC and SDC) and fatty acid (C10 and C12) penetration enhancers. Sugar conjugation increases the CMC since carbon atoms to which the sugar is attached, and carbons between the sugar and the hydrophilic surfactant headgroup, have a weaker effect on the CMC. The CMC of a liposaccharide with structure **7** is easily adjusted by variation of the LAA alkyl chain length, and a single methylene group influences the CMC by a factor of 5. Therefore, if the efficacy and/or toxicity of a liposaccharide is related to the propensity to aggregate, it should be possible to modulate efficacy and/or toxicity with only minor alterations in the hydrophobic tail length.

**Thermodynamics of Micellization.** The enthalpy of micellization ( $\Delta H_{\text{mic}}$ ), the Gibbs free energy of micellization ( $\Delta G_{\text{mic}}$ ), and the entropy of micellization ( $\Delta S_{\text{mic}}$ ) are important thermodynamic parameters which assist in understanding micelle formation. Using calorimetry to study the micelli-

(38) Bai, G.; Wang, J.; Yan, H.; Li, Z.; Thomas, R. K. Thermodynamics of molecular self-assembly of two series of double-chain singly charged cationic surfactants. *J. Phys. Chem. B* **2001**, *105*, 9576–9580.  
 (39) Klevens, H. B. Critical micelle concentrations as determined by refraction. *J. Phys. Colloid Chem.* **1948**, *52*, 130–148.  
 (40) Klevens, H. B. Structure and aggregation in dilute solutions of surface-active agents. *J. Am. Oil Chem. Soc.* **1953**, *30*, 74–80.

(41) Tanford, C. *The Hydrophobic Effect: formation of micelles and biological membranes*, 2nd ed.; Wiley: New York, 1980.  
 (42) Shinoda, K. *Colloidal Surfactants: some physico-chemical properties*; Academic Press: New York, 1963.  
 (43) Birdi, K. S. *Thermodynamics of Micelle Formation. Micellization, Solubilization, and Microemulsions*; Plenum Press: New York, 1977; pp 151–169.

**Table 2.** Thermodynamic Parameters of Micellization

compound	T (°C)	$\Delta G_{\text{mic}}^a$ (kJ/mol)	$\Delta H_{\text{mic}}^b$ (kJ/mol)	$T\Delta S_{\text{mic}}^c$ (kJ/mol)
7b	37	-20.4	-1.14	19.3
7c	37	-26.3	-4.91	21.4
7d	37	-32.2	-7.27	25.0
STC	37	-21.7 <sup>d</sup>	-1.99	19.7 <sup>d</sup>
C10 <sup>e</sup>	50	-19.6	-	-
SDC	37	-24.3 <sup>d</sup>	-4.43 <sup>f</sup>	19.8 <sup>d</sup>
C12	50	-26.3	-9.29	17.0
SDS	37	-27.5	-7.67 <sup>f</sup>	19.9

<sup>a</sup> Calculated from eq 3 using the CMC obtained via the van Os method. <sup>b</sup> Enthalpy difference (at the CMC obtained via the van Os method) between two lines fitted by linear regression to data well above and below the CMC in the  $\Delta H$  vs  $c$  plot (see Figure 1A). Values are the mean of three replicate titrations with a percent relative SEM of <5%. The 7b experiment was performed only in duplicate. <sup>c</sup> Calculated from eq 4. <sup>d</sup> Calculated for comparison. A low aggregation number means the value is only a coarse approximation.<sup>46</sup> <sup>e</sup> Type C enthalpogram<sup>69</sup> (see Figure S1 of the Supporting Information); therefore,  $\Delta G_{\text{mic}}$  was calculated using  $c_1$ , and estimates of  $\Delta H_{\text{mic}}$  and  $T\Delta S_{\text{mic}}$  are not possible. <sup>f</sup> Lit.  $\Delta H_{\text{mic}}$ : -4.8 kJ/mol for SDC (35 °C, 0.1 M NaCl),<sup>46</sup> -1.90 kJ/mol for SDS (25 °C, 0.1 M NaCl), and -11.80 kJ/mol for SDS (50 °C, 0.1 M NaCl).<sup>34</sup>

zation process has an advantage in that  $\Delta H_{\text{mic}}$  may be read directly from the  $\Delta H$  versus  $c$  plot. As illustrated in Figure 1A,  $\Delta H_{\text{mic}}$  is calculated as the enthalpy difference, at the CMC, between the two lines fitted by linear regression to data well above and below the CMC.<sup>35</sup> Estimates of  $\Delta H_{\text{mic}}$  for each penetration enhancer are listed in Table 2.

In terms of the classical phase separation and mass action models of micellization,<sup>31</sup> by making the assumptions that the degree of counterion binding of monomers and micelles is small and identical, the aggregation number ( $m$ , the number of monomer units which compose a micelle) is large, and the activity coefficients are close to unity, we can then estimate  $\Delta G_{\text{mic}}$  by<sup>34,44,45</sup>

$$\Delta G_{\text{mic}} = RT \ln x_{\text{CMC}} \quad (3)$$

where  $x_{\text{CMC}}$  is the CMC in mole fraction units. It should be noted that the assumption that  $m$  is large is not strictly applicable for bile salts SDC and STC.<sup>46</sup> To be able to compare the systems however, eq 3 was applied to all surfactants regardless of aggregation number.<sup>34,46</sup>

Values of  $\Delta G_{\text{mic}}$  calculated by eq 3 are listed in Table 2. All estimates of  $\Delta G_{\text{mic}}$  are negative, and for the series 7b–d, lengthening the LAA alkyl chain by a single methylene alters  $\Delta G_{\text{mic}}$  by -2.95 kJ/mol. This trend is displayed

(44) Mehrian, T.; de Keizer, A.; Korteweg, A. J.; Lyklema, J. Thermodynamics of micellization of *n*-alkylpyridinium chlorides. *Colloids Surf, A* **1993**, *71*, 255–267.

(45) Kiraly, Z.; Dekany, I. A thermometric titration study on the micelle formation of sodium decyl sulfate in water. *J. Colloid Interface Sci.* **2001**, *242*, 214–219.

(46) Garidel, P.; Hildebrand, A.; Neubert, R.; Blume, A. Thermodynamic characterization of bile salt aggregation as a function of temperature and ionic strength using isothermal titration calorimetry. *Langmuir* **2000**, *16*, 5268–5276.

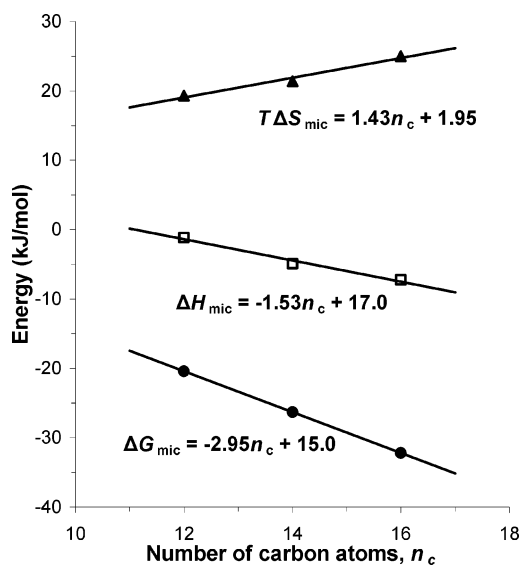


**Figure 3.** Variation of the thermodynamic parameters of micellization with the number of LAA carbon atoms ( $n_c$ ) for the series 7b–d: (▲)  $T\Delta S_{\text{mic}}$ , (□)  $\Delta H_{\text{mic}}$ , and (●)  $\Delta G_{\text{mic}}$ .

graphically in Figure 3. A similar contribution from each methylene to micellization was observed for *n*-alkylpyridinium chlorides in 0.1 M NaCl,<sup>44</sup> and a variety of other surfactants.<sup>29–31</sup>

The change in entropy  $\Delta S_{\text{mic}}$  can be obtained from the Gibbs–Helmholtz equation<sup>34</sup>

$$\Delta S_{\text{mic}} = (\Delta H_{\text{mic}} - \Delta G_{\text{mic}})/T \quad (4)$$

The entropy term  $T\Delta S_{\text{mic}}$  for each surfactant is listed in Table 2. The data in Table 2 indicate that large positive values of  $T\Delta S_{\text{mic}}$  are the main driving force for micellization, supported by a small exothermic enthalpy term. The large entropy gain on micellization can be explained by a number of theories,<sup>29</sup> the most generally accepted mechanism being the hydrophobic effect.<sup>29,34,47</sup> It suggests that alkyl groups induce an increase in water structure around themselves, and upon micellization, this structured water around each chain reverts to ordinary bulk water with a considerable gain in entropy.<sup>29</sup> An additional contribution to the entropy gain may be attributed to loss of hydration water molecules from the sugar moiety upon micellization, as observed for octyl glucoside<sup>48</sup> and sulfated sugar surfactants.<sup>26</sup>

For 7b–d, the contributions to  $T\Delta S_{\text{mic}}$  and  $\Delta H_{\text{mic}}$  per methylene are 1.43 and -1.53 kJ/mol, respectively (Figure 3). Thus, although  $T\Delta S_{\text{mic}}$  is the driving force for micellization, the contribution per methylene as the LAA alkyl chain is lengthened is approximately equal in entropy and enthalpy.

(47) Frank, H. S.; Evans, M. W. Free volume and entropy in condensed systems. III. Entropy in binary liquid mixtures; partial molal entropy in dilute solutions; structure and thermodynamics in aqueous electrolytes. *J. Chem. Phys.* **1945**, *13*, 507–532.

(48) Pastor, O.; Junquera, E.; Aicart, E. Hydration and micellization processes of *n*-octyl  $\beta$ -D-glucopyranoside in aqueous solution. A thermodynamic and fluorimetric study in the absence and presence of salts. *Langmuir* **1998**, *14*, 2950–2957.

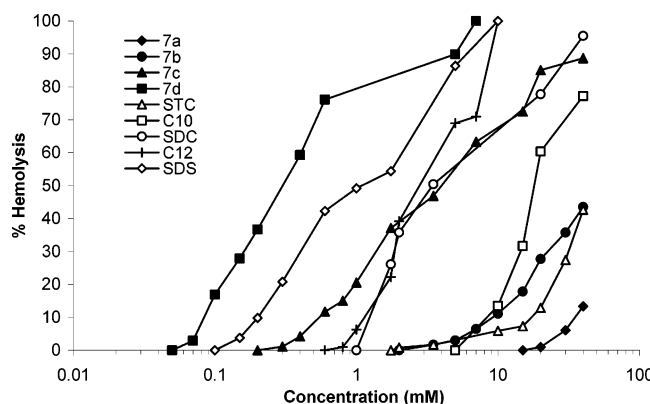


**Figure 4.** Percent hemolysis of human erythrocytes in PBS as a function of penetration enhancer concentration (pH 7.4, 37 °C, and incubation for 15 min). Data points are the mean of two to four experiments with a percent relative SEM of  $\leq 5\%$ . The C12 percent relative SEM  $\leq 10\%$ .

**Hemolytic Activity.** Penetration enhancers perturb membrane lipids and proteins and so may damage tissues.<sup>5</sup> Many penetration enhancers solubilize membranes by extracting membrane lipids to form mixed micelles, therefore enhancing drug absorption but causing significant membrane damage or even cell lysis.<sup>9,49,50</sup> In this study, hemolysis assays were used to determine the deleterious effects of the penetration enhancers.<sup>12–14,51</sup> Hemolysis assays estimate the membrane damage caused by a surfactant by measuring the amount of hemoglobin released from erythrocytes incubated with various concentrations of the surfactant. Human erythrocytes in PBS were incubated with various concentrations of a penetration enhancer for 15 min at 37 °C, and the concentration of released hemoglobin was expressed as the percentage of total hemoglobin. Figure 4 illustrates the hemolysis curves which were typically sigmoidal in shape, similar to those in other studies.<sup>12–14,51</sup> Hemolytic activity was observed over a concentration range spanning 3 orders of magnitude. The hemolytic activity of each enhancer is listed in Table 3 in terms of EC<sub>10</sub>, the concentration of enhancer required to cause 10% hemolysis.

The enhancers may be classified into three distinct groups (see Table 3 and Figure 4). The first group includes **7a**, **7b**, STC, and C10 which possess low hemolytic activity. C10 is used clinically as a penetration enhancer in suppositories,<sup>19,52</sup>

(49) Hirai, S.; Yashiki, T.; Mima, H. Mechanisms for the enhancement of the nasal absorption of insulin by surfactants. *Int. J. Pharm.* **1981**, *9*, 173–184.  
 (50) Murakami, T.; Sasaki, Y.; Yamajo, R.; Yata, N. Effect of bile salts on the rectal absorption of sodium ampicillin in rats. *Chem. Pharm. Bull.* **1984**, *32*, 1948–1955.  
 (51) Pillion, D. J.; Amsden, J. A.; Kensil, C. R.; Recchia, J. Structure–function relationship among *Quillaja* saponins serving as excipients for nasal and ocular delivery of insulin. *J. Pharm. Sci.* **1996**, *85*, 518–524.  
 (52) Motohiro, T.; Aramaki, M.; Tanaka, K.; Koga, T.; Shimada, Y.; Tomita, N.; Sakata, Y.; Fujimoto, T.; Nishiyama, T. Fundamental study on ceftizoxime suppository in adults and children. *Jpn. J. Antibi. **1985**, *38*, 3013–3056.*

**Table 3.** Concentrations of Penetration Enhancers Required To Cause 10% Hemolysis (EC<sub>10</sub>) of a Human Erythrocyte Suspension

compound	EC <sub>10</sub> <sup>a</sup> (mM)	comments <sup>b</sup>
<b>7a</b>	35.1	low hemolytic activity,
STC	17.3	show potential as
<b>7b</b>	9.39	biocompatible
C10	9.38	penetration enhancers
SDC	1.28	moderate hemolytic
C12	1.19	activity, SDC irritating
<b>7c</b>	0.589	to membranes <sup>53</sup>
SDS	0.204	strong hemolytic activity,
<b>7d</b>	0.0872	likely to cause damage <i>in vivo</i>

<sup>a</sup> Estimated from the data presented in Figure 4. <sup>b</sup> Based on comparison with conventional enhancers and literature data.

**Table 4.** IAM Chromatographic Capacity Factors (K<sub>IAM</sub>) of the Penetration Enhancers

compound	K <sub>IAM</sub> <sup>a</sup>	compound	K <sub>IAM</sub> <sup>a</sup>	compound	K <sub>IAM</sub> <sup>a</sup>
<b>7a</b>	0.13	<b>7d</b>	26.56	SDC	9.16
<b>7b</b>	8.27	STC	4.51	C12	9.22
<b>7c</b>	22.02	C10	6.88		

<sup>a</sup> Calculated using eq 2.

and STC has been reported to possess low cytotoxicity *in vitro*.<sup>53</sup> Therefore, **7a** and **7b** show potential as biocompatible penetration enhancers for drug delivery. A second group of enhancers, SDS and **7d**, exhibit strong hemolytic effects, and these penetration enhancers are likely to cause tissue damage *in vivo*. In between these two groups are **7c**, SDC, and C12 which possess EC<sub>10</sub> values of  $\sim 1$  mM. SDC is generally considered an effective enhancer but is irritating to membranes.<sup>13</sup>

On the basis of the hemolytic activity data, the conclusion can be made that liposaccharides that contain  $\leq 12$  carbon atoms in the LAA moiety (i.e., n<sub>c</sub>  $\leq 12$ ) are likely to possess suitable toxicity profiles (e.g., **7a** and **7b**). Nevertheless, liposaccharides with slightly longer alkyl chains (n<sub>c</sub>  $\leq 14$ ) may be suitable because no significant morphological changes were seen in the gastrointestinal tracts of rats treated orally with **7c** (100 mg/kg).<sup>10</sup> This finding concurs with Lee's statement<sup>5</sup> that hemolytic activity may not always be extrapolated directly to the effects a penetration enhancer has on mucosal cells. For example, acylcarnitines, which produced significant hemolysis *in vitro*,<sup>54,55</sup> caused no significant damage to rat mucosal tissue even after prolonged exposure at concentrations higher than that used in the

(53) Axelrod, H. R.; Kim, J. S.; Longley, C. B.; Lipka, E.; Amidon, G. L.; Kakarla, R.; Hui, Y. W.; Weber, S. J.; Choe, S.; Sofia, M. J. Intestinal transport of gentamicin with a novel, glycosidic drug transport agent. *Pharm. Res.* **1998**, *15*, 1876–1881.  
 (54) Cho, K. S.; Proulx, P. Lysis of erythrocytes by long-chain acyl esters of carnitine. *Biochim. Biophys. Acta* **1969**, *193*, 30–35.  
 (55) Cho, K. S.; Proulx, P. Studies on the mechanism of hemolysis by acyl carnitines, lysocerithins and acyl cholines. *Biochim. Biophys. Acta* **1971**, *225*, 214–223.

hemolysis assay.<sup>56</sup> Such discrepancies arise because the gastrointestinal tract is protected *in vivo* by a mucous layer and possesses mechanisms for recovery from trauma,<sup>8</sup> unlike the erythrocytes used in the hemolysis assay. Hemolysis assays are useful, however, for predicting the rank order of enhancer effects,<sup>8</sup> and when they are considered in conjunction with reference compounds (e.g., C10, C12, SDC, STC, and SDS) and *in vivo* data, it is predicted that liposaccharides with  $n_c \leq 14$  are worthy of further examination as penetration enhancers.

### Correlation between Hemolytic Activity and Micellar Aggregation.

Sugar conjugate **7b** ( $EC_{10} = 9.39$  mM) is 1 order of magnitude less hemolytic than the structurally similar fatty acid C12 ( $EC_{10} = 1.19$  mM). This could be explained by the increase in CMC induced by sugar conjugation since **7b** has a CMC of 20.2 mM whereas C12 aggregates at 3.15 mM. Effectively, **7b** has 10 carbon atoms in its hydrophobic tail, and comparison of **7b** ( $EC_{10} = 9.39$  mM and CMC = 20.2 mM) with C10 ( $EC_{10} = 9.38$  mM and CMC = 37.8 mM) reveals similar  $EC_{10}$  and CMC values. In fact, for all the penetration enhancers that have been studied, CMC values are indicative of hemolytic activity, and there exists a good negative correlation ( $R^2 = 0.90$ ) between hemolytic potency [ $\log(1/EC_{10})$ ] and  $\log$  CMC (Figure 5A). Such a correlation between CMC and hemolytic activity was also observed by Moni et al.<sup>57</sup> for a study limited to three surfactants. For the series **7b-d** alone, an improved correlation was obtained (Figure 5A,  $R^2 = 0.99$ ), which indicates that the CMC is a reliable indicator of liposaccharide hemolytic potency.

Despite this finding, it is unlikely that penetration enhancer micelles are responsible for the onset of hemolysis because the CMC values for all enhancers are greater than the concentrations at which hemolysis first appears (see Table 1 and Figure 4). In fact, for all enhancers other than STC and **7d**, the  $EC_{10}$  value is less than  $c_1$ , which indicates that hemolysis can reach levels of greater than 10%, prior to the inception of aggregation. These findings suggest that penetration enhancer monomers are responsible for the initial disruption of the erythrocyte membrane, as reported by Moni et al.<sup>57</sup> Although hemolysis is not attributed to micelles, correlation with CMC is observed because for amphiphilic molecules the formation of micelles is an expression of the lipophilicity of the molecules in aqueous solution.<sup>58</sup> Penetration enhancer lipophilicity should influence the membrane partitioning of monomers and will therefore affect the hemolytic potency. Correlation between penetration enhancer lipophilicity and hemolytic potency has been noted previ-

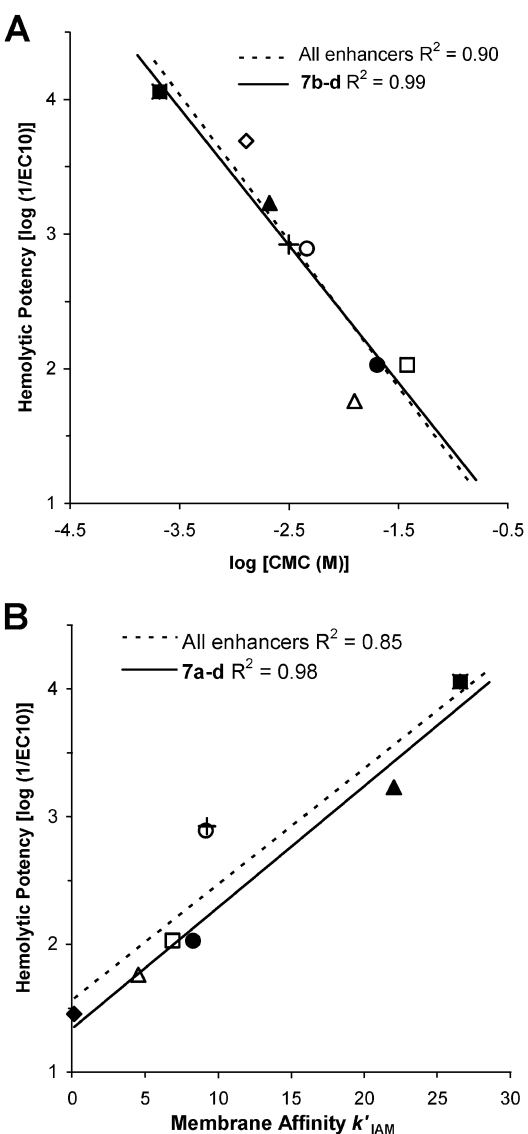


**Figure 5.** (A) Relationship between hemolytic potency [ $\log(1/EC_{10})$ ] and  $\log$  CMC for all penetration enhancers ( $y = -1.09x + 0.23$ ) and **7b-d** ( $y = -1.02x + 0.36$ ): (●) **7b**, (▲) **7c**, (■) **7d**, (△) STC, (□) C10, (○) SDC, (+) C12, and (◊) SDS.  $EC_{10}$  was in units of moles per liter. (B) Relationship between hemolytic potency [ $\log(1/EC_{10})$ ] and  $K'_{IAM}$  for all penetration enhancers ( $y = 0.091x + 1.564$ ) and **7a-d** ( $y = 0.095x + 1.340$ ): (◆) **7a**, (●) **7b**, (▲) **7c**, (■) **7d**, (△) STC, (□) C10, (○) SDC, and (+) C12.  $EC_{10}$  was in units of moles per liter.

ously,<sup>9,13</sup> and a reduction in enhancer lipophilicity reduced the level of membrane damage.

**Immobilized Artificial Membrane Chromatography.** To examine the relationship between penetration enhancer membrane partitioning and hemolytic activity, we employed immobilized artificial membrane (IAM) chromatography.

(56) Fix, J. A.; Engle, K.; Porter, P. A.; Leppert, P. S.; Selk, S. J.; Gardner, C. R.; Alexander, J. Acylcarnitines: drug absorption-enhancing agents in the gastrointestinal tract. *Am. J. Physiol.* **1986**, 251, G332–G340.

(57) Moni, R. W.; Parsons, P. G.; Quinn, R. J.; Willis, R. J. Critical micelle concentration and hemolytic activity. A correlation suggested by the marine sterol, halistanol trisulfate. *Biochem. Biophys. Res. Commun.* **1992**, 182, 115–120.

(58) Devinsky, F.; Lacko, I.; Mlynarcik, D. Aggregation Properties as a Measure of Lipophilicity in QSAR Studies of Antimicrobially Active Amphiphiles. *QSAR in Design of Bioactive Compounds*; J. R. Prous Science: Barcelona, 1992; pp 233–247.

IAM chromatography<sup>59,60</sup> is a chromatographic method that mimics solute partitioning into fluid membranes that are chemically and physically similar to the phospholipid bilayers of biological membranes. (The stationary phase is composed of phosphatidylcholine analogues covalently bonded to an inert silica support at high molecular densities.) IAM chromatography has been used to estimate the extent of membrane partitioning,<sup>61,62</sup> and the partitioning of the solute into an immobilized membrane is generally governed by lipophilicity, hydrogen bonding, and ion pairing interactions.<sup>63</sup> This is significant since a penetration enhancer can affect a drug's efficacy, toxicity, pharmacokinetic properties, absorption, distribution, metabolism, and excretion through these interactions. The chromatographic capacity factor ( $k'_{\text{IAM}}$ ) for a solute obtained by IAM chromatography correlates with its  $K_{\text{IAM}}$  partitioning coefficient for partitioning between the mobile phase and the IAM-bonded phase ( $k'_{\text{IAM}} = \Phi K_{\text{IAM}}$ , where  $\Phi = V_s/V_m$ , which is the stationary phase to the mobile phase ratio of the column), and ultimately with its  $K_m$  that describes the distribution of the enhancer between an aqueous phase and the phospholipid bilayers of actual biological membranes. Essentially, an increase in  $k'_{\text{IAM}}$  indicates an increase in the level of membrane interaction (affinity).

Several penetration enhancers involved in this study had a strong affinity for the IAM stationary phase, resulting in very long chromatographic retention times when a purely aqueous mobile phase was used. For these compounds, isocratic elutions with various concentrations of an organic modifier (acetonitrile) were used to obtain workable retention times that were then extrapolated to purely aqueous conditions by linear regression (see Figure S2B of the Supporting Information which illustrates the procedure using **7c** as an example). On the basis of the  $k'_{\text{IAM}}$  values that were obtained (Table 4), liposaccharide **7a** exhibited little membrane affinity in contrast to **7c** and **7d** which revealed a strong binding to the IAM stationary phase. The affinity of **7b** for IAM was weaker than that of C12, which indicated that conjugation of GlcA to the fatty acid core decreased membrane affinity. However, the surfactant SDS could not be eluted under the conditions that were employed. This may

be due to its strong affinity for the IAM stationary phase. In the past, IAM chromatography has been extensively used as a preliminary screen for drug membrane permeability across Caco-2-cells,<sup>64</sup> intestinal tissue,<sup>60</sup> human skin,<sup>65</sup> and the blood–brain barrier.<sup>62,66</sup> Although surfactants have been characterized by the technique,<sup>67</sup> to the best of our knowledge, this is the first report to employ IAM chromatography to study the interaction of penetration enhancers with membranes.

**Correlation between Hemolytic Activity and Membrane Affinity.** As stated in the previous section, membrane partitioning of a penetration enhancer can influence a drug's pharmacological effects and pharmacokinetic properties. For this reason, we wanted to see how well the  $k'_{\text{IAM}}$  values would correlate with the hemolytic activity of penetration enhancers. As illustrated in Figure 5B, there is positive correlation ( $R^2 = 0.85$ ) between  $k'_{\text{IAM}}$  values and hemolytic potency [ $\log(1/\text{EC}_{10})$ ] for all penetration enhancers. For the series **7a–d** alone, an even stronger correlation ( $R^2 = 0.98$ ) was observed. These results indicate that IAM chromatography can be used as a method to predict the hemolytic potency of penetration enhancers.

**Structure–Property Relationship.** It is valuable to predict the hemolytic activity of a penetration enhancer based on structure, rather than to correlate an experimentally measured parameter with hemolytic potency. Knowledge of such structure–property relationships would greatly assist in penetration enhancer design. Figure 6 illustrates the relationship between the hemolytic potency [ $\log(1/\text{EC}_{10})$ ] and  $n_c$  for liposaccharides **7a–d**. An increase in the length of the LAA alkyl chain significantly increased hemolytic potency, and similar relationships have been observed for *N*-alkylpolymethylenediamine surfactants.<sup>14</sup> The ability to control hemolytic activity with variation in  $n_c$  is an advantage of synthetic penetration enhancers, as opposed to enhancers based solely on natural agents for which such control is lacking.<sup>51,68</sup>

**Conclusions.** We examined the hemolytic activity of a series of amphiphilic penetration enhancers and found that

(59) Pidgeon, C.; Venkataram, U. V. Immobilized artificial membrane chromatography: supports composed of membrane lipids. *Anal. Biochem.* **1989**, *176*, 36–47.

(60) Ong, S.; Liu, H.; Pidgeon, C. Immobilized-artificial-membrane chromatography: measurements of membrane partition coefficient and predicting drug membrane permeability. *J. Chromatogr., A* **1996**, *728*, 113–128.

(61) Yang, C. Y.; Cai, S. J.; Liu, H.; Pidgeon, C. Immobilized artificial membranes: screens for drug–membrane interactions. *Adv. Drug Delivery Rev.* **1997**, *23*, 229–256.

(62) Braddy, A. C.; Janaky, T.; Prokai, L. Immobilized artificial membrane chromatography coupled with atmospheric pressure ionization mass spectrometry. *J. Chromatogr., A* **2002**, *966*, 81–87.

(63) Austin, R. P.; Davis, A. M.; Manners, C. N. Partitioning of ionizing molecules between aqueous buffers and phospholipid vesicles. *J. Pharm. Sci.* **1995**, *84*, 1180–1183.

(64) Pidgeon, C.; Ong, S.; Liu, H.; Qiu, X.; Pidgeon, M.; Dantzig, A. H.; Munroe, J.; Hornback, W. J.; Kasher, J. S.; et al. IAM chromatography: an in vitro screen for predicting drug membrane permeability. *J. Med. Chem.* **1995**, *38*, 590–594.

(65) Ong, S.; Liu, H.; Qiu, X.; Bhat, G.; Pidgeon, C. Membrane partition coefficients chromatographically measured using immobilized artificial membrane surfaces. *Anal. Chem.* **1995**, *67*, 755–762.

(66) Reichel, A.; Begley, D. J. Potential of immobilized artificial membranes for predicting drug penetration across the blood–brain barrier. *Pharm. Res.* **1998**, *15*, 1270–1274.

(67) Ward, R. S.; Davies, J.; Hodges, G.; Roberts, D. W. Applications of immobilised artificial membrane chromatography to quaternary alkylammonium sulfobetaines and comparison of chromatographic methods for estimating the octanol–water partition coefficient. *J. Chromatogr., A* **2003**, *1007*, 67–75.

(68) Hu, Z.; Tawa, R.; Konishi, T.; Shibata, N.; Takada, K. A novel emulsifier, Labrasol, enhances gastrointestinal absorption of gentamicin. *Life Sci.* **2001**, *69*, 2899–2910.

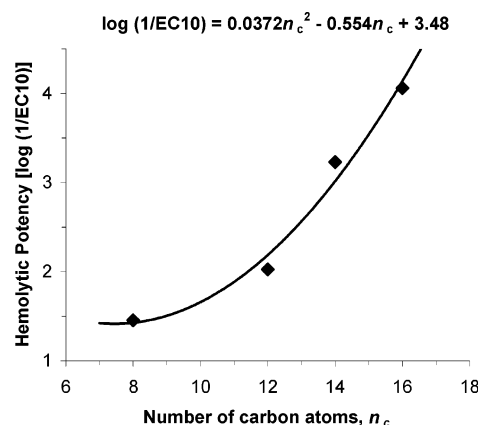


**Figure 6.** Relationship between hemolytic potency [ $\log(1/\text{EC}_{10})$ ] and the number of LAA carbon atoms ( $n_c$ ) for the series **7a–d**.  $\text{EC}_{10}$  was in units of moles per liter.

monomers, not micelles, were responsible for the onset of hemolysis. Nevertheless, a negative correlation was observed between CMC values and the hemolytic potency of the penetration enhancers. This correlation was attributed to the fact that the CMC is a surrogate measure of lipophilicity,<sup>58</sup> and lipophilicity should affect the membrane partitioning of a penetration enhancer and therefore influence hemolysis. The membrane partitioning of each penetration enhancer was determined by IAM chromatography, and  $k'_{\text{IAM}}$  values exhibited a positive correlation with hemolytic potency. IAM chromatography therefore shows promise as a technique that can be used to accurately predict the hemolytic activity of

(69) Bijma, K.; Engberts, J. B. F. N.; Blandamer, M. J.; Cullis, P. M.; Last, P. M.; Irlam, K. D.; Soldi, G. Classification of calorimetric titration plots for alkyltrimethylammonium and alkylpyridinium cationic surfactants in aqueous solutions. *J. Chem. Soc., Faraday Trans.* **1997**, *93*, 1579–1584.

(70) Matsuoka, K.; Maeda, M.; Moroi, Y. Micelle formation of sodium glyco- and taurocholates and sodium glyco- and taurodeoxycholates and solubilization of cholesterol into their micelles. *Colloid Surf., B* **2003**, *32*, 87–95.

(71) Kolthoff, I. M.; Stricks, W. Solubilization of dimethylaminoazobenzene in solutions of detergents. II. Effect of electrolytes on the critical concentration and the solubilization of dimethylaminoazobenzene, Orange OT, and trans-azobenzene in detergent solns. *J. Phys. Colloid Chem.* **1949**, *53*, 424–454.

penetration enhancers. The CMC and hemolytic activity of liposaccharides (**7**) can be modulated by *minor* alterations to hydrophobic tail length. Using hemolytic activity as a guide, it was determined that liposaccharides with  $n_c \leq 12$  are biocompatible; however, liposaccharides with slightly longer hydrophobic tails ( $n_c \leq 14$ ) could be suitable considering prior *in vivo* results.<sup>10</sup>

### Abbreviations Used

C10, sodium decanoate; C12, sodium dodecanoate; CMC, critical micelle concentration; DIEA, diisopropylethylamine; DMF, *N,N*-dimethylformamide; EC<sub>10</sub>, concentration required to cause 10% hemolysis; GlcA, D-glucopyranuronic acid; HBTU, 2-(1*H*-benzotriazol-1-yl)-1,1,3,3-tetramethyluronium hexafluorophosphate; HPLC, high-performance liquid chromatography; IAM, immobilized artificial membrane; ITC, isothermal titration microcalorimetry;  $k'_{\text{IAM}}$ , IAM chromatography capacity factor;  $K_{\text{IAM}}$ , IAM partition coefficient;  $K_m$ , membrane partition coefficient; LAA, lipoamino acid;  $n_c$ , number of carbon atoms in the LAA or fatty acid; PBS, phosphate-buffered saline; PE, penetration enhancer; SDC, sodium deoxycholate; SDS, sodium dodecyl sulfate; SEM, standard error of the mean; STC, sodium taurocholate; THF, tetrahydrofuran.

**Acknowledgment.** We thank Mr. Alun Jones (Institute for Molecular Bioscience, The University of Queensland) for accurate mass measurements and A/Prof Ian Gentle (School of Molecular and Microbial Sciences, The University of Queensland) for helpful discussions. B.P.R. acknowledges The University of Queensland for a Ph.D. scholarship and Alchemia Pty. Ltd. for a Ph.D. studentship.

**Supporting Information Available:** Synthesis of series **b** and **d**, the  $\Delta H$  versus  $c$  plot for C10 (type C enthalpogram),<sup>59</sup> additional discussion which describes the relationship between log CMC and  $n_c$ , a sample IAM chromatogram indicating retention time reproducibility ( $SD < 2\%$ ), and a figure which illustrates the method used to determine  $k'_{\text{IAM}}$  equivalent to purely aqueous elution conditions. This material is available free of charge via the Internet at <http://pubs.acs.org>.

MP049964D